ASSESSMENT OF MULTI-DIMENSIONAL COMPONENT OF MARS WITH AIR-WATER CROSS FLOW EXPERIMENT

Jin-Hwa Yang and Dong-Jin Euh
Thermal Hydraulics Safety Research Division
Korea Atomic Energy Research Institute
989-111, Daedeok-daero, Yuseong-gu, Daejeon 305-600, Korea
f1yjh@kaeri.re.kr; djeuh@kaeri.re.kr

Chi-Jin Choi, Hyoung-Kyu Cho* and Goon-Cherl Park
Nuclear Thermal-Hydraulic Engineering Laboratory, Seoul National University
Gwanak 599, Gwanak-ro, Gwanak-gu, Seoul 151-742, Korea
chijin2g@snu.ac.kr; chohk@snu.ac.kr; parkgc@snu.ac.kr

ABSTRACT

Recently, high precision and high accuracy analysis on multi-dimensional thermal hydraulic phenomena in a nuclear power plant have been dealt as state-of-the-art issues. System analysis code, MARS-MultiD, also adapted a multi-dimensional module to simulate them more accurately. Even though it was applied to deal the multi-dimensional phenomena, but implemented models in that are one-dimensional empirical models based on one-dimensional pipe experimental results. Prior to the application of the multi-dimensional simulation tools, however, the constitutive models implemented in the code for a two-phase flow need to be carefully validated, such as the wall and interfacial shear models.

In particular, in a Direct Vessel Injection (DVI) system, the injected Emergency Core Coolant (ECC) on the upper part of the downcomer interacts with the lateral steam flow during the reflood phase in the Large-Break Loss-Of-Coolant-Accident (LBLOCA). The interaction between the falling film and lateral steam flow induces a multi-dimensional two-phase flow. The prediction of this flow behavior plays a key role in determining the amount of coolant that can be used as core cooling. Therefore, the wall and interfacial shear models which are suitable to deal this phenomenon need to be validated with multi-dimensional experimental results.

In this paper, the two-phase cross flow experiments simulating the multi-dimensional phenomenon which occurs in the upper downcomer will be introduced. As a result, two-dimensional local liquid film velocity and thickness data were produced and the wall shear model of the MARS-MultiD in the annular flow regime was validated. The validation results indicated the wall shear model implemented in the MARS-MultiD is needed to be modified for analysis of two-phase cross flow and it will be used to improve that model as a further work.

KEYWORDS
Two-phase cross flow, liquid film velocity, liquid film thickness, MARS-MultiD, wall shear stress model.

* Corresponding author

1. INTRODUCTION

The high precision and high accuracy analysis on multi-dimensional thermal hydraulic phenomena in nuclear power plant has been dealt as state-of-the-art issues. The integrated project in European Union (EU), Nuclear Reactor Safety (NURESAFE) simulation platform with NEPTUNE-CFD [1] and the Consortium for Advanced Simulation of LWRs (CASL) [2] in United State of America (USA) are well-known activities regarding the actualization of a thermal-hydraulic two-phase computational fluid dynamics (CFD) analysis. They are aimed to simulate or predict the two-phase phenomena more accurately than one-dimensional codes, which have limitations in dealing with multi-dimensional phenomena. These works in computational codes should be performed together with multi-dimensional experimental study and verification and validation (V&V) activities of constitutive models are essential to apply the multi-dimensional modules on the two-phase phenomena. The MARS-MultiD [3] which was developed by Korea Atomic Energy Research Institute (KAERI) is a system analysis code to deal with the multi-dimensional thermal hydraulic phenomena in nuclear power plant. The constitutive models of it, for instance, the wall and interfacial friction factor models should be also validated with multi-dimensional experimental results before using them.

In the downcomer of the reactor pressure vessel, especially, in the Advanced Power Reactor 1400 (APR1400) which has direct vessel injection (DVI) lines as an emergency core cooling system, connected to about 2.1m above the cold-leg center, multi-dimensional two-phase flows may occur in a Loss-of-Coolant-Accident (LOCA). The accurate prediction of them is of high relevance to evaluation of the integrity and soundness of the reactor core. In the case of upper part of the downcomer, highly convective steam flow exists and in particular, in a DVI system, the injected Emergency Core Coolant (ECC) on the upper part of the downcomer interacts with the lateral steam flow during the reflood phase in the Large-Break LOCA (LBLOCA) as shown in Fig. 1 [4]. The injected ECC falls down along the downcomer wall as a liquid film and the interaction between the falling film and lateral steam flow induces a two-phase cross flow. It determines the bypass flow rate of the emergency core coolant and subsequently, the reflood coolant flow rate. Therefore, an accurate prediction of this phenomenon is important for evaluating the core cooling capability of the safety injection system. Its flow pattern can be defined as an annular flow/annular mist flow according to the one-dimensional flow regime map due to its high void fraction and high gas velocity. However, different from the one-dimensional annular flow, it has two-dimensional characteristics apparently and a multi-dimensional analysis is required for the prediction of this phenomenon.

Recently, an experiment was performed by KAERI to investigate the two-dimensional film flow phenomena which simulated the two-phase cross flow in the downcomer. A 1/10 scaled down rectangular shape test section was devised to simulate an unfolded downcomer. The depth-averaged Particle Image Velocimetry (PIV) method was applied to measure the two-dimensional liquid film velocity. This measurement method identifies local velocity data averaged along the depth direction of a thin liquid film. And the ultrasonic thickness gauge was applied to measure the liquid film thickness. Using these two experimental methods, the local liquid film velocity and thickness data of two-phase cross flow were produced.

This paper introduces the experimental facility and the local measuring methods. Also, the experimental data of two-phase cross flow will be presented. With these local experimental data, the wall shear model in the MARS-MultiD was assessed. Through the validation activity, the ways to advance the multi-dimensional modules in the MARS-MultiD will be discussed.

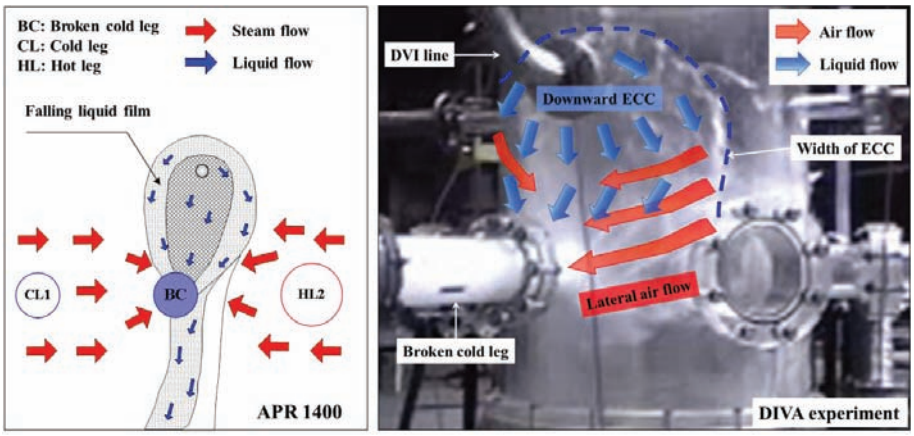

Figure 1. Two-phase Cross Flow in Upper Downcomer [4].

2. TWO-PHASE CROSS FLOW EXPERIMENT

2.1. Features of Experiments

2.1.1. Experimental facility

An experimental facility was devised to measure the local film velocity and thickness of the two-phase cross flow which used air and water as working fluids, as shown in Fig. 2-(a). The air was selected as a gas phase fluid instead of steam to separate the condensation or heat transfer effect from the hydraulic effect. The test section was made as an unfolded-shaped upper downcomer with a 1/10 reduced scale of APR 1400 because the local measurement methods which were adopted in this study are not suitable to cylindrical geometry.

The experimental facility includes a water supply system to simulate the falling liquid film and an air supply system to provide transverse gas flow. The water was injected through a nozzle which had an inner diameter as 21.6 mm from a storage tank by a pump. The inner diameter was scaled down from an inlet nozzle of the DVI line of APR1400. The injected water impinged on one side of the test section of which dimensions are 1.4 m × 0.62 m × 0.025 m (W × H × D) and made a two-dimensional liquid film falling down on the wall (Fig. 2-(b)). The air was injected by a blower along the 152.4 mm (6-inch diameter) pipe. The air was uniformly distributed by a perforated plate in the expansion section. The injected air and falling water makes a two-dimensional film flow. At the end of the test section, the two phases were separated by a separator. After that, the water returned to the storage tank through the drain line at the bottom of the test section and the separator. The air exited through the top of the separator.

2.1.2. Experimental conditions

In order to define test conditions, the modified linear scaling method, which was developed by Yun et al. [5], was adopted. This model preserves Wallis parameter, as shown in Eq. (1), between model and proto type.

$$j_k^* = \frac{\dot{m}_k}{\rho_k A_{flow}} \left[\frac{\rho_k}{(\rho_f - \rho_g) g D_{gap}} \right]^{1/2} \quad (1)$$

According to this scaling method, the liquid and gas velocities were divided by the square root of the scaled length ratio and the reduced velocities were employed as test conditions. In the prototype reactor, it is assumed that the ECC injected at a 2 m/s water velocity through the DVI line, and the velocity of lateral steam varied from 15 m/s to 45 m/s [6]. Following the modified linear scaling method, 0.63 m/s of inlet liquid velocity and 5~15 m/s of lateral air velocity were selected as experimental conditions. The instruments used for measuring the boundary variables are listed below; a SPONSLOER turbine flow meter which had measuring uncertainty as 0.28 % was used to measure inlet mass flow of water. An OVAL 76.2 mm (3 inches) vortex flow meter that had 0.41 % measuring uncertainty was used to measure volumetric inlet flow rate of air. And ROSEMOUNT gauge pressure transmitters were used to measure absolute pressures of test section and air pipe which had measuring uncertainties as 0.36 % and 0.86 %, respectively. Temperatures in water pipe line, air pipe line and test section were measured by T-type thermocouples which had measuring uncertainty under 0.5 ℃.

For local measurement of the two-dimensional film flow, a 30 mm × 30 mm (w × h) control volume was selected and the test section was divided into 19 × 7 virtual control volumes as shown in Fig. 3-(a) and Fig. 4. By using a traverse system, the local measurement instrument, such as LASER system and high speed camera, were traversed to cover the whole control volumes. Detail introduction to the local measurement methods, ultrasonic thickness gauge and depth-averaged PIV, will be treated in the following sections.

2.2. Local Measurement Methods for Two-dimensional Film Flow

2.2.1. Ultrasonic thickness gauge for local liquid film thickness measurement

The ultrasonic thickness gauge is a widely used method to measure the thickness of the material. The pulse-echo type ultrasonic thickness gauge defines thickness from the round-trip time of an ultrasonic wave. It is following as Eq. (2).

$$\delta_f = \frac{c_f(T)\Delta t}{2} \tag{2}$$

where δ_f is the liquid film thickness, c_f is the sound speed in water, T is the temperature of water, and Δt is the round trip time of an ultrasonic wave. Figure 3 shows the measurement method and a raw data graph. The liquid film thickness data were measured on every cross point of the horizontal and vertical lines in Fig. 3-(a). The electric signal has two peak points by the reaching pulse after reflecting each interface. The first peak came from the interface between the acrylic test section and the liquid film and the second peak was from the one between the liquid film and air. Therefore, the gap of these two peaks is proportional to the thickness of the liquid film and with the traveling wave velocity. And then, the film thickness can be calculated. This method has bias errors less than 0.5 % of the measured thickness due to the measurement error of the temperature and time resolution accuracy [7]. The maximum value of total uncertainty of the measured thickness with precision errors was less than 3.63 % when the measured thickness was within 2.52 mm.

2.2.2. Depth-averaged PIV method for local liquid film velocity measurement

The PIV method for measuring velocity of single-phase flow in a pipe or duct is able to produce local measurement data which are useful for validation of multidimensional T/H codes and CFD codes. A conventional PIV methodology is the sheet PIV that uses a thin sheet laser beam created by a cylindrical concave lens. It produces velocity data on the area that was passed through by the incident laser. In this

method, the laser sheet is supposed to penetrate into the liquid film through the film edge and travels parallel to the film surface.

However, there are two limitations to apply the sheet PIV method for the two-phase cross flow experiment. One is that the thickness of the liquid film flow is too narrow for a laser sheet to be transmitted. The other is that reflection on the oscillated film boundary and attenuation effect of the light causes a deterioration of the laser intensity. Due to these limitations, the conventional sheet PIV could not provide reliable local velocity data for this experiment.

To overcome these difficulties in applying the sheet PIV method, the depth-averaged PIV method which applied cone-shape laser from a round concave lens was developed uniquely in this study. It used the incident laser which illuminates the liquid film in front of the acryl test section in diagonal directions and it was able to yield averaged velocity data along the depth direction. As shown in Fig. 4, two lasers excited the fluorescent particles, 1~20 μm polymethyl metacrylate (PMMA)-Rhodamine B-particles, in the liquid film and high speed camera took pictures of particles' movement in front of the test section. The specification of the lasers was a 523 nm-10 W power of Diode-Pumped Solid State Laser (DPSSL) and the one of the high speed camera was PHANTOM v211 which has 40 ns timing accuracy.

With the depth-averaged PIV method, it was possible to maintain the light intensity since it is not disturbed by the oscillation on the boundary nor attenuation of laser source since the light does not travel along the liquid film. However, the reflection effect on the interface between film and air was remained. In order to reduce that, a long pass filter was installed in front of the high speed camera lens (Fig. 4). The fluorescent particles were excited by a 532 nm laser source and emitted reflection light up to 570 nm range. If the reflected laser light on the interface can be cut off under the 560 nm region, the reflection effect can be also eliminated. After taking 500 pairs filtered images on every measuring control volume in Fig 4., the adaptive PIV method was applied to produce velocity vectors by Dynamic Studio v3.31. This is a PIV analysis software using cross-correlation between two particle movement images which have time interval. In this experiment, 500 μs was used as the interval time between two images, then the frame rate was 1000 FPS (frames per second) and the frame resolution was 512 × 512 pixels. The uncertainty analysis as to the depth-averaged PIV was carried out by a validation experiment [8] and that was quantified as 5.96 % with a 95 % confidence level.

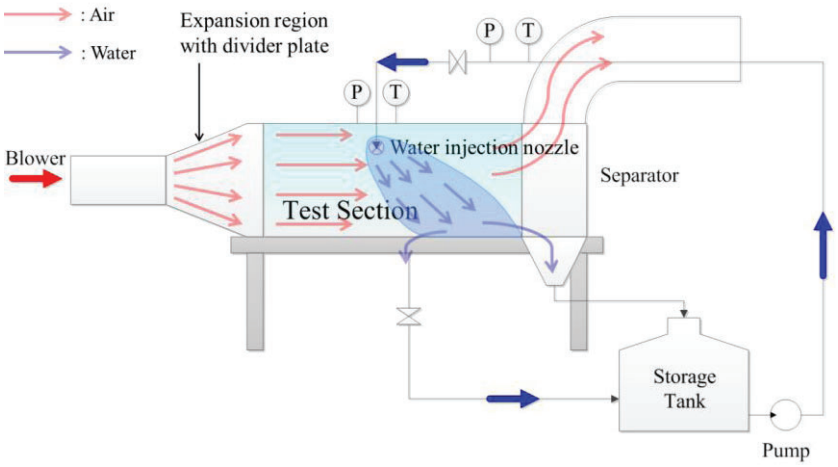

(a) Flow directions of working fluids

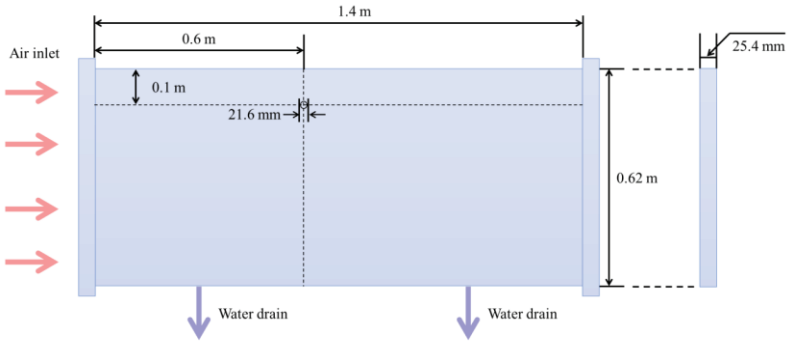

(b) Test section

Figure 2. Schematics of Experimental Facility.

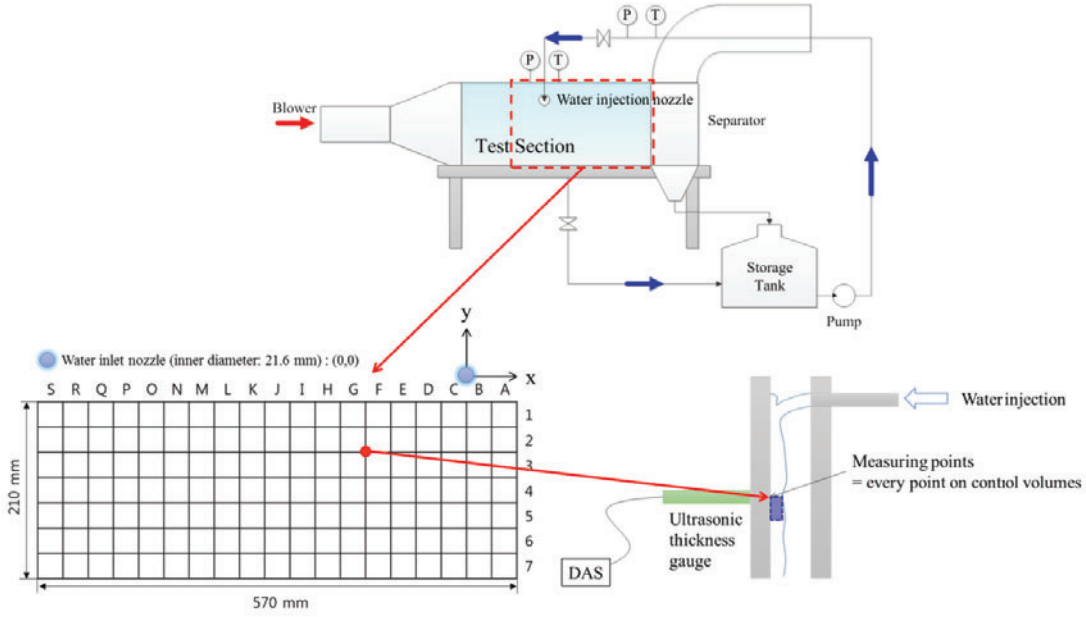

(a) Measurement method

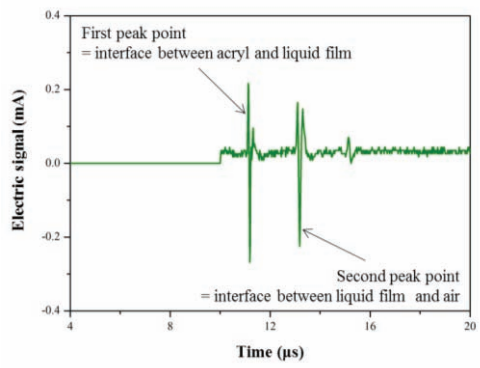

(b) Raw data

Figure 3. Ultrasonic Thickness Gauge for Liquid Film Thickness Measurement.

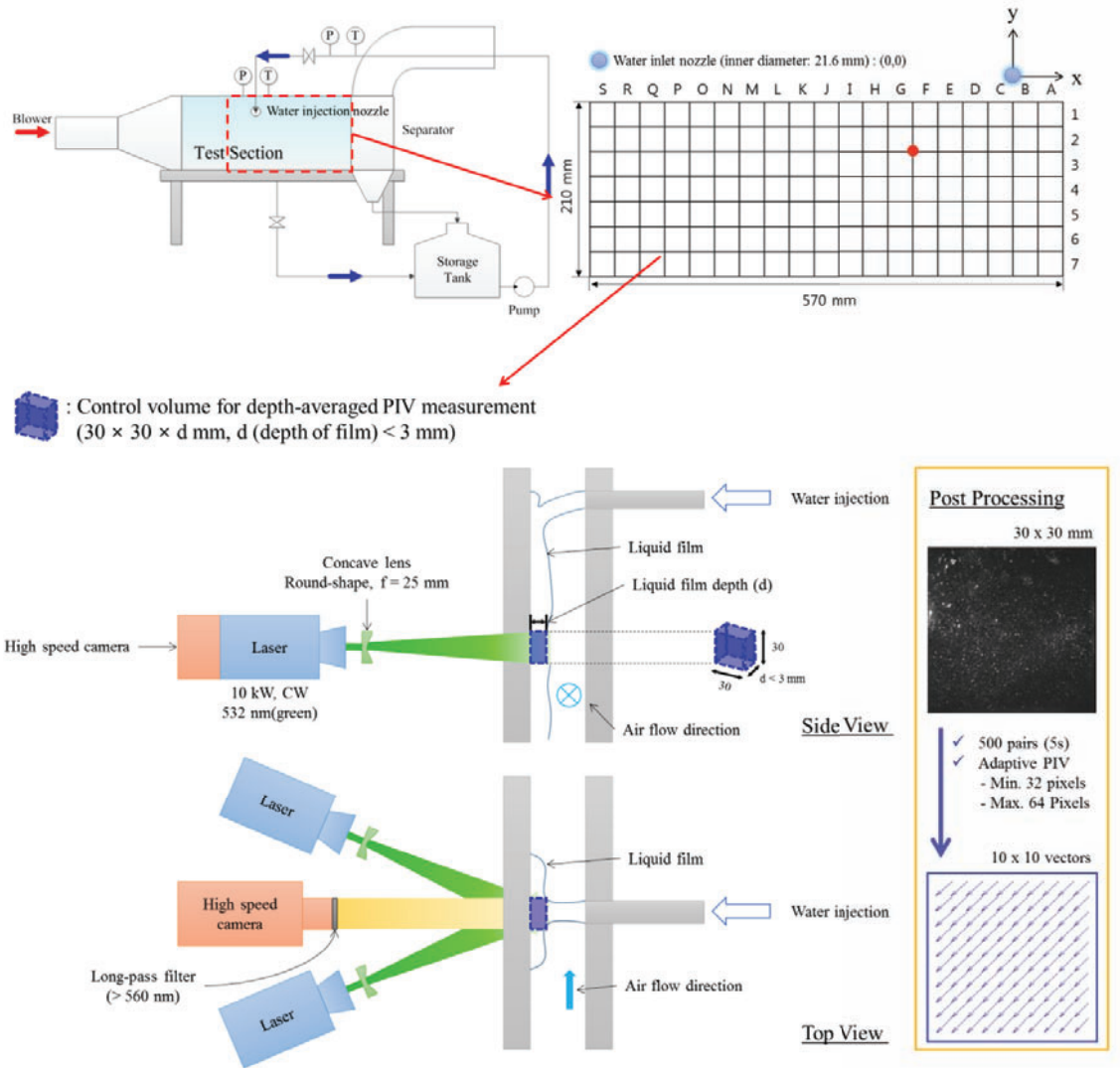

Figure 4. Depth-averaged PIV Method for Measurement of Liquid Film Velocity.

3. EXPERIMENTAL RESULTS

3.1. Classification of Test Conditions

In the present experiment, the gas velocity varies from 5 m/s to 15 m/s and due to this wide range of the lateral air velocity, different physical phenomena were observed as it increased. Figure 5 shows the liquid film shape change with increase of lateral air velocity. The experiment without air injection was also considered as a reference case. Under the condition of which velocities are lower than 7 m/s, the widths of falling film were remained stationary. However, in the cases with the velocities larger than 9 m/s, the falling films shifted to the downstream of air cross flow with entrainment. In the case with 15 m/s, there were several flow patterns on the film flow; thin film, thick film, entrainment and de-entrainment [8]. In this study, the test conditions were classified into three phases; at first, one without lateral air, secondly, cases without entrainment (v_g = 5 ~ 7 m/s) and finally, cases with entrainment (v_g = 9 ~ 15 m/s).

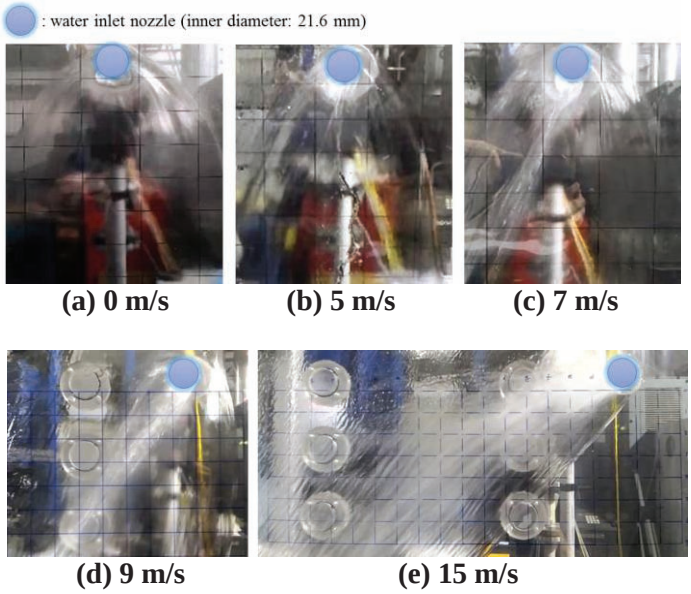

Figure 5. Liquid Film Shape Change with Increase of Lateral Air Velocity

3.2. Two-phase Cross Flow without Entrainment

The interaction between the falling liquid film and the lateral air induces momentum transfer through the interface. Figure 6 shows the liquid film velocity vectors and thickness data according to the increase of lateral air velocity. In the graph, the vectors mean liquid film velocity and the gradation of contour means thickness distribution. The water inlet nozzle was positioned at (0 mm, 0 mm). Without the lateral air injection (0 m/s), the velocities of liquid film are almost symmetric along the centerline of the inlet nozzle (x = 0 mm). In the cases with the lateral air (5 and 7 m/s), the maximum velocity vectors are displaced to the exit side of the test section. The mass errors were under 0.17 % at 0 m/s, 5.22 % at 5 m/s and 13.7 % at 7 m/s which were comparison results between the water inlet mass flow rate measured by the turbine flow meter and the mass flow rate by local measurements integrated along the upper boundary of the measurement region (y = -60 mm) [8].

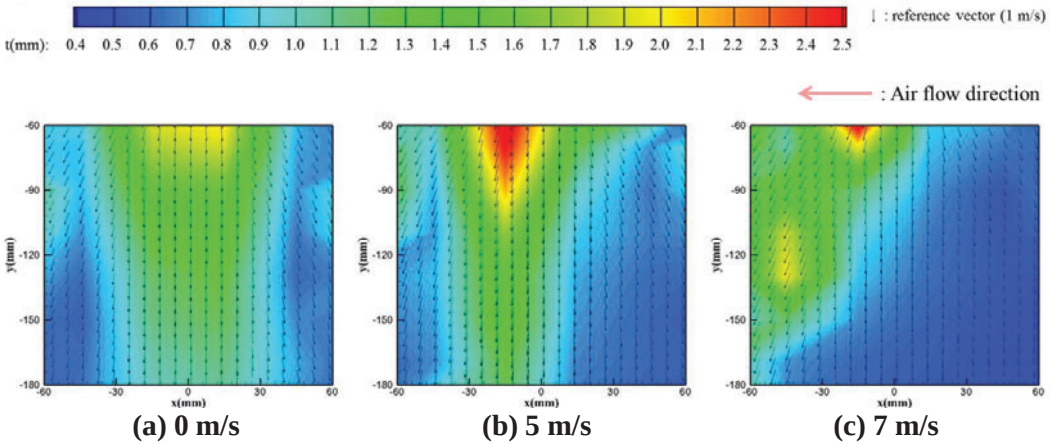

Figure 6. Local Liquid Film Velocity and Thickness of Two-phase Cross Flow without Entrainment

3.3. Two-dimensional Film Flow with Entrainment

Figure 7 shows the local liquid film velocity and thickness data when the entrainment occurred due to high lateral velocity. In these results, the vectors indicate liquid film velocities and the contour does thickness distribution. In the cases with the lateral air velocity larger than 9 m/s, the entrainment phenomena were observed on the interface. And then, the shapes of liquid film were more shifted to the downstream of air cross flow.

Meanwhile, the flow patterns which were observed on the interface can be divided into four regions; thin film, thick film, entrainment and de-entrainment [8]. By dividing the two-phase cross flow as the four flow patterns, it was possible to define the characteristics of the liquid film flow with lateral air injection with force balances between the wall and interfacial shear stresses. These local experimental results can be used to validate the wall and interfacial shear models in the multi-dimensional module in the system analysis codes, for example, MARS-MultiD.

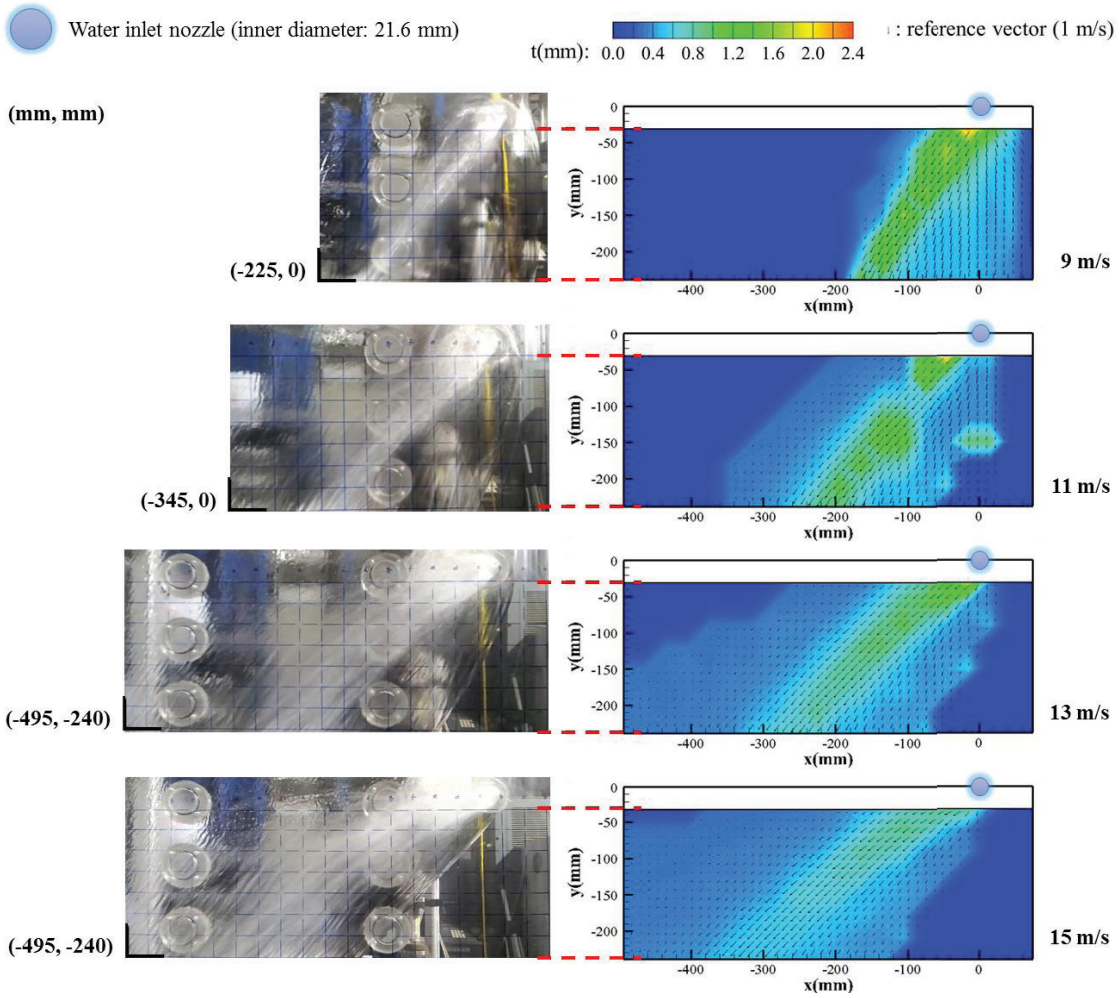

Figure 7. Local Liquid Film Velocity and Thickness of Two-phase Cross Flow with Entrainment

4. VALDATION WITH MARS-MULTID

4.1. Modeling of Two-dimensional Film Flow Experiment

The nodalization of test section for MARS-MultiD is presented in Fig. 8. The numbers of the volumes were 189 with 21 volumes × 9 volumes (x × y). The water was injected into the center of the 89th volume which was simulated as an impingement spot. The lateral air was simulated with four different velocities (0 m/s, 5 m/s, 11 m/s, 15 m/s). The liquid film thickness was calculated by the liquid fraction in each volume, and the liquid film velocity was calculated in each junction connected with volumes.

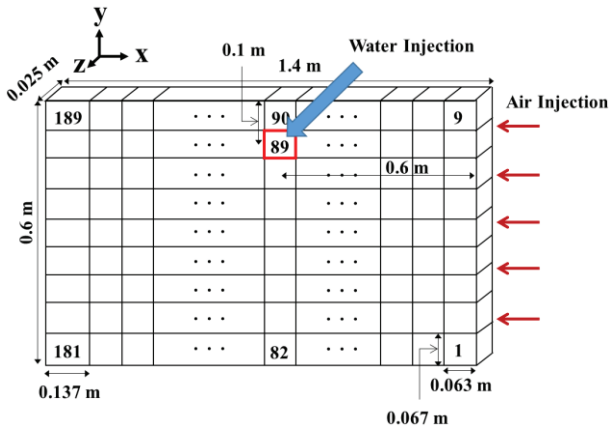

Figure 8. Nodalization of Test Section

4.2. Calculation Results and Analysis

The local variables such as the liquid film velocity and thickness could be obtained from MARS-MultiD calculation. Figure 9 shows the change of the void fraction distribution with increase of lateral air velocity and the liquid fractions can be assumed as liquid film thicknesses. According to the increase of air velocity, the liquid film moved toward the outlet side of the test section due to the increase of the interfacial shear stress. In order to validate the adequacy of MARS-MultiD calculation, these variables obtained by the code were compared with the experimental results. As shown in Fig. 10, the local liquid film velocities from calculations and experiments at the marked region with red lines in Fig. 9 were compared. The reference case (v_g = 0 m/s) shows that the magnitudes of the liquid film velocity calculated by the MARS-MultiD was overestimated than experimental ones. With the lateral air velocities, the magnitudes of the liquid film velocity were also much larger than those of experimental data. Not only the magnitudes, but the directions of the liquid film velocities were different. The calculated results were much more toward to the outlet side of the test section. It could be due to the interfacial shear stress, but the results were not independent from the wall shear stress. Therefore, the separated effect between wall and interfacial shear stress should be assessed at first.

The variation of the local liquid film thickness on a horizontal line (from x = -62.5 mm to x = 62.5 mm) at y = -50 mm is presented in Fig. 11. In both cases (0 m/s, 5 m/s), the calculated liquid film thicknesses were underestimated than experimental data. It also indicated that the wall shear stress calculated by MARS-MultiD was under-predicted. In order to validate shear stress models implemented in the MARS-MultiD, the prior concern is the modification of the wall shear stress model in the annular flow regime in a condition without the effects of the interfacial shear stress.

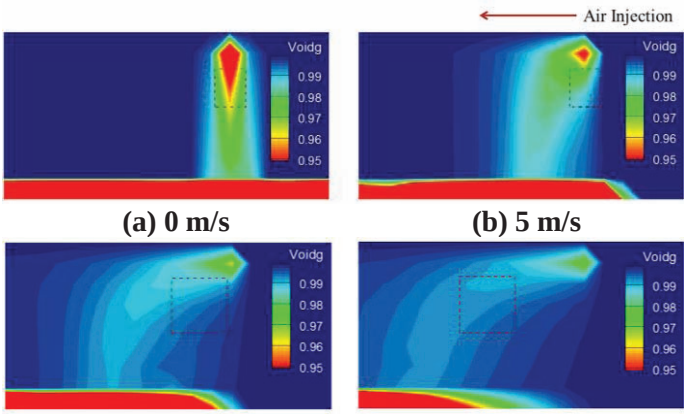

(a) 0 m/s (b) 5 m/s

(c) 11 m/s (d) 15 m/s

Figure 9. Change of Void Fraction Distribution with Increase of Lateral Air Velocity

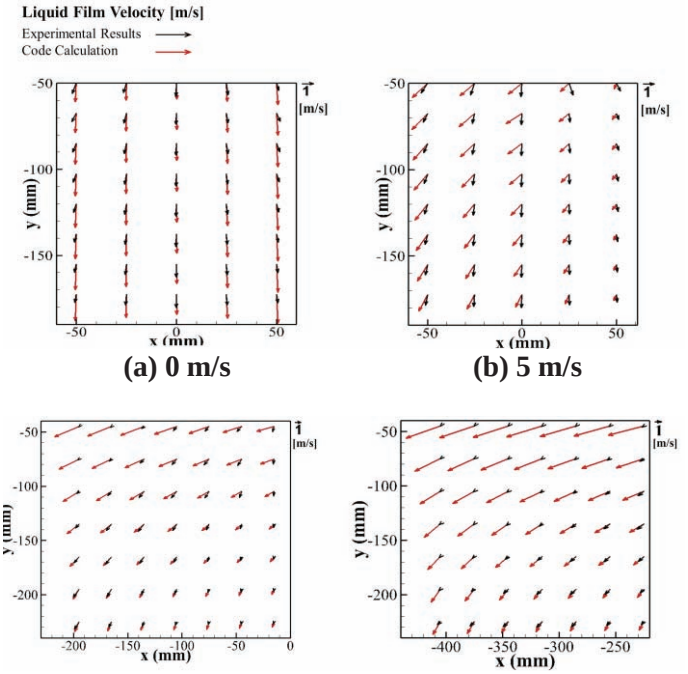

(a) 0 m/s (b) 5 m/s

(c) 11 m/s (d) 15 m/s

Figure 10. Comparisons of Liquid Film Velocity Vectors with Increase of Lateral Air Velocity

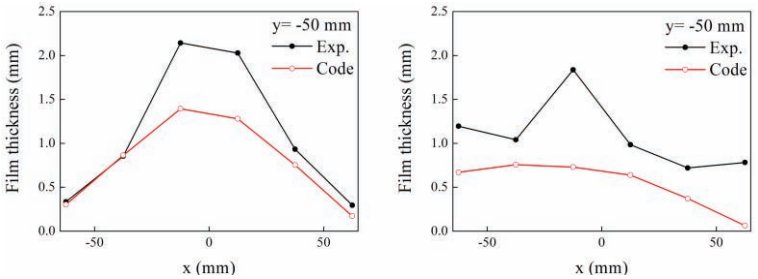

(a) 0 m/s (b) 5 m/s

Figure 11. Comparisons of Liquid Film Thickness with Increase of Lateral Air Velocity

4.3. Challenges for Modification of Wall Shear Stress Model

In order to modify the wall shear stress model, the reference case (v_g = 0 m/s) was chosen since the effect of the interfacial shear stress can be ignored. As a result, the initial velocities calculated by MARS-MultiD were overestimated than experimental results. There could be several reasons and additional modifications should be considered for validation of the wall shear model because the MARS-MultiD cannot treat local physical phenomena directly, for example, the impingement on the wall and the hydraulic jump due to the surface tension on the boundary of liquid film.

The initial velocities (v_i) calculated by MARS-MultiD on the upper boundary of control volume (y = -50 mm) can be simply assumed as shown in Eq. (3),

$$v_i = v_0 - at = v_0 - \left(a_{wall\ shear} - g\right)t \tag{3}$$

The velocity after impingement (v_0) was accelerated by a force which was balanced between gravity force and wall shear stress. As shown in Fig. 10-(a), in the case without air injection, the results with default condition of MARS-MultiD present overestimated liquid film velocities. It is due to the two reasons; one is that the velocity after impingement was overestimated and the other is that the wall shear stress was under-predicted.

4.3.1. Effect of impingement on the wall

If the inlet water impinged on the wall, the energy of liquid flow decreased following the pressure distribution as shown in Fig. 12. And the velocity after impingement (v_0) was calculated by Eq. (4) with energy distribution [9].

$$v_0 = \frac{1 - erf\left(\sqrt{\log 2}\right)}{erf\left(\sqrt{\log 2}\right)} v_c \tag{4}$$

where, the contact velocity was $v_c = \left(v_{in}^{\ 2} + 2gh\right)^{1/2}$ and h was the falling length of liquid through the gap of the duct before contacting on the wall as shown in Fig. 12. When the liquid was injected with 0.63 m/s, the liquid velocity falling down on the wall after impingement was about 0.54 m/s. However, the MARS-MultiD cannot treat impingement phenomena since there isn't the impingement model in the multi-dimensional module. If the impingement effect can be estimated by MARS-MulitD, the over-predicted initial velocity (v_i) would be modified.

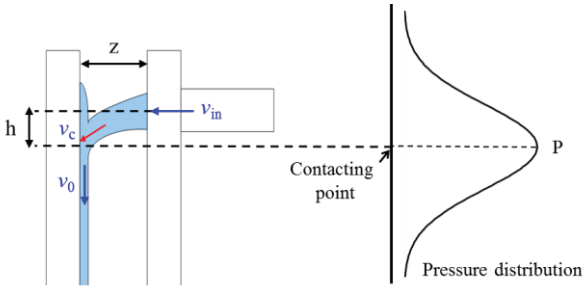

Figure 12. Effect of Impingement on Liquid Film Velocity

4.3.2. Effect of two-phase frictional pressure gradient

The two-phase frictional pressure gradient in the MARS-MultiD which is based on the RELAP5/MOD3 [10] is calculated from Lockhart-Martinelli model [11] and Heat Transfer and Fluid Flow Service (H.T.F.S) correlation [12]. The two-phase frictional pressure gradient plays significant role to define wall shear stress in the code since it is proportional to the shear stress terms ($\tau_{w,k}$) of each phase [13].

Before the analysis of two-phase cross flow, the validation activity with multi-dimensional experimental data is necessary since these model and correlations were developed by one-dimensional experimental studies. The aforementioned local experimental data of two-phase cross flow were used to calculate the wall shear stresses by the Eq. (5) and (6). The control volume for calculation was defined as following the size of measuring control volume; 30 mm × 30 mm (w × h). And then, without air injection condition (v_g = 0 m/s), the wall shear stresses from experimental results and code calculation were compared as shown in Fig. 13.

$$-\frac{\int_A \tau_{wf,x}\, dA}{A} = \sum_{in\_x} \left(\rho_f U_{f\_face} \times U_n\right) - \sum_{out\_x} \left(\rho_f U_{f\_face} \times U_n\right) \tag{5}$$

$$-\frac{\int_A \tau_{wf,y}\, dA_1}{A_1} + \rho_f gH - \rho_g gH = \sum_{in\_y} \left(\rho_f U_{f\_face} \times U_n\right) - \sum_{out\_y} \left(\rho_f U_{f\_face} \times U_n\right) \tag{6}$$

The comparison results indicated that the MARS-MultiD underestimated the wall shear stress than the results from calculation by the experimental data. As a previous study according to an application of the wall shear model of the RELAP5/MOD3 in the annular flow regime, Yao and Ghiaasiaan [14] noted the H.T.F.S correlation significantly under-predicted the liquid film thickness and it was because the wall shear stress was underestimated. And they suggested the Wallis' correlation which made the best fitting line with experimental data as a wall shear model in the annular flow regime. The aforementioned wall shear stress results which were calculated by local experimental data also informed the similar tendency. If the H.T.F.S correlation in the MARS-MultiD is replaced with the Wallis' correlation in the annular flow regime, the modified results could be produced.

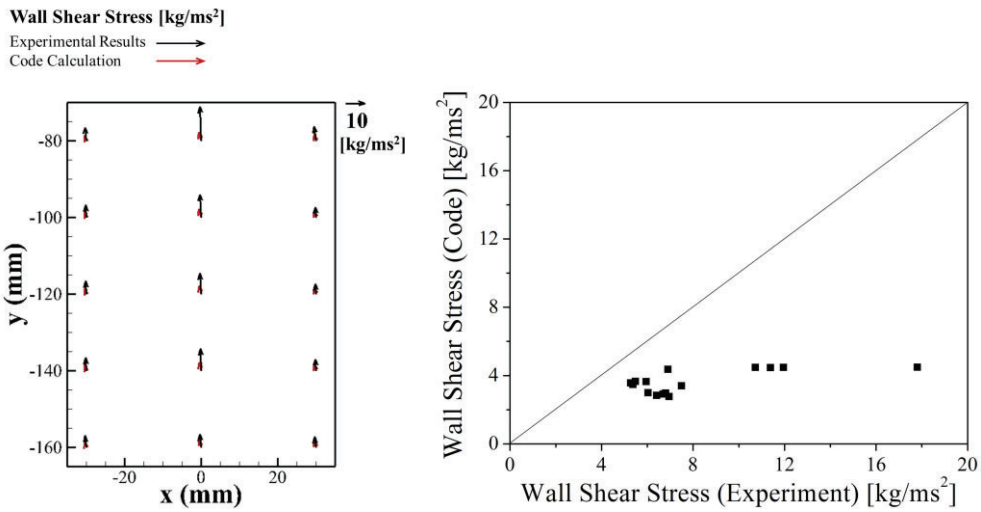

Figure 13. Comparison Results of Wall Shear Stresses

5. Conclusion

The experimental study of the two-phase cross flow was carried out with local measurement methods; depth-averaged PIV and ultrasonic thickness gauge. Using these local measurement methods, the two-dimensional liquid velocity and thickness data were obtained. These experimental results were used to validate the wall shear stress model in the multi-dimensional module of the system analysis code, MARS-MultiD. The validation results will be applied to modify the wall shear model of the MARS-MultiD, and then, the interfacial shear model of the MARS-MultiD is also expected to be validated with local data of two-phase cross flow experiments.

ACKNOWLEDGMENTS

This work was supported by the National Research Foundation of Korea (NRF) grant funded by the Korea government (MSIP) (No. 2012M2A8A4004176).

REFERENCES

1. P. Emonot, A. Souyri, J. Gandrille, and F. Barre, "CATHARE-3: A new system code for thermal-hydraulics in the context of the NEPTUNE project," *Nuclear Engineering and Design*, **241**, pp. 4476-4481 (2011).
2. T. M. Smith, et al., "Thermal Hydraulic Simulations, Error Estimation and Parameter Sensitivity Studies in Drekar::CFD," Sandia National Laboratories, CASL-U-2013-0203-001 (2013).
3. Korea Atomic Energy Researcher Institute, "MARS Code Manual Volume I: Code Structure, System Models, and Solution Methods," KAERI/TR-2812/2004 (2007).
4. H.K. Cho, B.J. Yun, C.-H. Song and G.C. Park, "Experimental Study for Multidimensional ECC Behaviors in Downcomer Annuli with Direct Vessel Injection Mode during the LBLOCA Reflood Phase," *Journal of Nuclear Science and Technology*, **42**(6), pp. 549–558 (2005).
5. B.J. Yun, H.K. Cho, Song, C.-H. Song and G.C. Park, "Scaling for the ECC bypass phenomena during the LBLOCA reflood phase," *Nuclear Engineering and Design*, **231**, pp. 315-325 (2004).
6. Korea Atomic Energy Researcher Institute, "Post-test Analysis for the APR1400 LBLOCA DVI Performance Test Using MARS," KAERI/TR-2137/2002 (2002).
7. D.J. Euh, S.T. Lee, J.H. Yang and S. Kim, "Application of uncertainty analysis to high precision thermo-hydraulic experimental methods". *Transactions of the Korean Nuclear Society Spring Meeting*, Jeju, Korea (2014).
8. J.H. Yang, H.K. Cho, S. Kim, D.J. Euh and G.C. Park, "Experimental study on two-dimensional film flow with local measurement methods," *Nuclear Engineering and Design*, **under review** (2015).
9. C.V. Tu and D.H. Wood, "Wall Pressure and Shear Stress Measurements Beneath an Impinging Jet," 1996, *Experimental Thermal and Fluid Science*, **13**, pp. 364-373 (1996).
10. RELAP5-3D Code Development Team, "RELAP5-3D Code Manual Volume I: Code Structure, System Models and Solution Methods," INEEL-EXT-98-00834, Revision 2.4 (2005).
11. R.W. Lockhart and R.C. Martinelli, "Proposed calculation of data for isothermal two-phase, two-component flow in pipes," *Chem. Eng. Prog.*, **45,** pp. 39-48 (1949).
12. RELAP5-3D Code Development Team, "RELAP5-3D Code Manual Volume IV: Models and Correlations," INEEL-EXT-98-00834, Revision 2.4, Revision 2.4 (2005).
13. D. Chisholm, "A theoretical basis for the Lockhart-Martinelli correlation for two-phase flow, *Int. J. Heat Mass Transfer*, **10**, pp. 1767-1778 (1967).
14. G.F. Yao and S.M. Ghiaasiaan "Wall friction in annular-dispersed two-phase flow," *Nuclear Engineering and Design*, **163** pp. 149-161 (1996).